IEEE Access
Multidisciplinary | Rapid Review | Open Access Journal

Received March 24, 2019, accepted April 17, 2019, date of publication April 30, 2019, date of current version May 21, 2019.

*Digital Object Identifier 10.1109/ACCESS.2019.2913888*

# A Stochastic Optimization Approach for Spectrum Sharing of Radar and LTE Systems

**MINA LABIB[1], ANTHONY F. MARTONE[2], VUK MAROJEVIC[3], JEFFREY H. REED[1], AND AMIR I. ZAGHLOUL[1,2]**

[1]Wireless@Virginia Tech, Bradley Department of Electrical and Computer Engineering, Virginia Tech, Blacksburg, VA 24061, USA
[2]U.S. Army Research Laboratory, Adelphi, MD 20783, USA
[3]Department of Electrical and Computer Engineering, Mississippi State University, Mississippi State, MS 39762, USA

Corresponding author: Mina Labib (mlabib@vt.edu)

This work was supported in part by the U.S. Army Research Laboratory.

**ABSTRACT** This paper proposes a chance-constrained stochastic optimization technique that enables effective coexistence between LTE-Unlicensed base stations and radars in a shared spectrum. The optimization problem is formulated to guarantee the minimum performance criteria for radar operation, and at the same time, allows the LTE-Unlicensed base station to control its transmit power to maximize the performance for the serving LTE-Unlicensed device. The proposed power control mechanism results in significant reduction of the required protection distance (3.9% of the one imposed by regulations) between the radar and the LTE-Unlicensed network for the two to effectively coexist in a shared spectrum.

**INDEX TERMS** LTE-unlicensed, LAA, LTE-U, radar systems, coexistence, spectrum sharing, stochastic optimization, chance-constrained optimization, power control, cognitive radars.

## I. INTRODUCTION

Billions of people rely on wireless communications technology and this dependence will continue to grow. As such, data traffic demand is expected to increase 8x from 2015 to 2020 [1]. Recent studies have shown that, except for the spectrum used for wireless communications, most portions of the spectrum are underutilized [2]. To satiate the need of the ever-growing wireless communications industry, regulatory groups are considering spectrum sharing technology that would allow communications system to effectively share the wireless channel with other RF systems [3]. One example of a spectrum sharing initiative is the DARPA (Defense Advanced Research Projects Agency) SSPARC (Shared Spectrum Access for Radar and Communications) program, which promotes research and development for spectrum sharing between communications and radar systems [4]. Several bands in the United States allow spectrum sharing, such as the 5150-5925 MHz, which is called Unlicensed National Information Infrastructure (U-NII) band.

In parallel to ongoing research and regulation, cellular network operators are extending the operation of LTE (Long Term Evolution) into the 5 GHz unlicensed spectrum, which is called LTE-Unlicensed. Currently, there are 3 versions of LTE-Unlicensed: LTE-U, LAA (License Assisted Access) and MulteFire [5]. The 5 GHz band is currently accessed by various radar systems, in addition to wireless local area networks (WLAN), which are also referred to as Wi-Fi systems. There are different radar types that operate in the 5 GHz band; these radars are either ground-based (scanning or tracking), shipborne, or airborne. The radiolocation radars are the main ones spanning the frequency range 5250-5850 MHz, the aeronautical radio-navigation radars operates within the frequency range 5350-5460 MHz, the maritime radio-navigation radars operate within the frequency band 5470-5650 MHz, and the Terminal Doppler Weather (TDWR) radars operate within the frequency range 5600-5650 MHz [6]. Despite the number of wireless users in 5 GHz, the band offers opportunities for communications because of the geographically sparse and temporally sporadic use of radar services. Accordingly, there is a need to develop innovative sharing techniques to mitigate the effect of potential and imminent interference issues between radar and communications systems, where our focus is on LTE-Unlicensed systems.

### A. RELATED WORK

There is a variety of spectrum sharing research that has been investigated for radar and communications systems coexistence. As shown in [7], the approaches for radar and communications systems can be broadly classified based on which

The associate editor coordinating the review of this manuscript and approving it for publication was Bilal Alatas.

system is responsible for avoiding creating interference to the other system.

One set of approaches is through employing joint radar and communications system spectrum sharing techniques. In [8], Bhat *et al.* introduce the concept of bandwidth sharing between multimodal radar and a communications system. A multimodal radar has the ability to vary its bandwidth (and accordingly its resolution) based on its current needs and allows the communications system to use the remaining bandwidth. The priority for the radar is determined using fuzzy logic and the priority for the communications system was assumed to be constant. Bandwidth sharing is also investigated for radar performance trade off using multi-objective optimization [9]. In that work, the radar bandwidth is estimated to maximize the joint SINR (signal-to-interference-plus-noise ratio) and range resolution objective functions based on spectrum sensing information. This technique has been shown to mitigate mutual interference while preserving radar performance. This concept was recently extended to consider radar priority for moving target indication [10]. Gogineni *et al.* [11] propose to design an OFDM (Orthogonal Frequency Division Multiplexing) waveform for both the multimodal radar and a communications system by assigning OFDM sub-carriers based on maximizing the radar detection performance and the communications system channel capacity. The previous set of approaches assume the possibility of changing the radar type or sharing information between the radar and the communications systems, which may not be a practical solution, given the fact the most of the radar types in the 5 GHz are operated by military agencies.

Another set of approaches is based on making the communications system responsible for avoiding interference to the radar systems by employing cognitive radio at the communications system side. The term ''cognitive radio'' refers to a system that has the ability to sense the surrounding RF environment, make short-term predictions, and dynamically adjust its transmitting parameters. These capabilities are used by a communications system that acts as a secondary user when sharing the spectrum with radars. The first example is the dynamic frequency selection (DFS) mandated by the Federal Communications Commission (FCC) for devices operating in the 5 GHz band. DFS is a mechanism that is specifically designed to avoid causing interference to non-IMT (International Mobile Telecommunications) systems, such as radars. The DFS requirements in the United States can be summarized as follows [12]:

- Sensing bandwidth: The device must sense radar signals in 100% of its occupied bandwidth.
- Channel availability check time: The device must monitor the channel for 60 s before using it.
- In-service monitoring: The device must continuously monitor the channel during operation and must vacate the channel within 10 s (called Channel Move Time) once the radar system start transmitting. During these 10 s, the device is only allowed 200 ms for normal transmission.
- Detection threshold: This is the received power level (measured at the communications system device) when averaged over 1 $\mu s$ referenced to a 0 dBi antenna:
  - $-62$ dBm: For devices with maximum EIRP less than 200 mW (23 dBm) and an EIRP spectral density of less than 10 dBm/MHz (10 mW/MHz)
  - $-64$ dBm: For devices that do not meet the above requirements for relaxed sensing detection.
- Detecting radar: Once the radar has been detected, the operating channel must be vacated. The device must not utilize the channel for 30 minutes, which is called the Non-occupancy Period.

The NTIA (National Telecommunications and Information Administration) developed an analysis to determine the trade-off between the DFS detection threshold and the potential aggregate interference from Wi-Fi devices in the 5 GHz through Monte-Carlo simulations [13], which led to determining the DFS detection threshold. There is several other research works in the literature based on employing cognitive radio at the communications systems side. Paisana *et al.* [14] investigate using a Radio Environment Map (REM) to enhance the spectrum awareness for communications systems sharing the frequency band with radars. In [15], Um *et al.* explore using multiple transmit antennas at the communications system side for sharing the spectrum with radars in the 5 GHz band, while still employing DFS and adhering to the regulatory constraints of the maximum transmit power. Saruthirathanaworakun *et al.* [16] introduce a spectrum sharing algorithm to address the coexistence issue between an OFDM communications system and a rotating radar, where the basic concept is that the communications system can utilize the period when the antenna beam of the rotating radar is not within the range of the communications system transmission. They show that communications systems can achieve a significant increase in the downlink throughput if they can tolerate the discontinuous transmission. Wang *et al.* [17] investigate and validate the feasibility of adjacent-channel coexistence of an LTE system and an air traffic control radar (with a rotating main beam) in the L-band through system-level simulation. Reference [18] analyzes the impact of interference from Wi-Fi transmitters on the ground-based radar operating in the 5.6 GHz band, using a simplified model for the radar antenna pattern. Hessar and Roy [19] provide characterization of radar-Wi-Fi coexistence as a function of different system parameters and analyze the physical distance needed between the two systems to coexist with each other. However, they assume that the Wi-Fi system transmits at the maximum power level.

Most of the work in the literature does not consider the fact that communications systems have the ability to adapt their transmission power when sharing the spectrum with radars. A power-control-based algorithm was provided in [20] for the coexistence between a rotating radar and a cellular system in adjacent channels. However, the analysis is limited to rotating antenna radars, where the rate of rotation is known at the

base station. Krishnan *et al.* [21] analyze the coexistence between radar and communications systems in the 3.5 GHz band through downlink power control at the communications system. However, the analysis is limited to shipborne naval radars, so they assume that the radar antenna gain is always in the direction of the communications system, and they do not consider the effect of radar interference on the communications system.

A non-intrusive approach, where the radar and communications system operate and adapt independently needs to deal with uncertainties in terms of operation and, particularly, RF activity. There are two sets of approaches that are usually used to capture the uncertainty in the parameters of an optimization problem: the deterministic approach or the statistical approach. For the set of deterministic approaches, the optimization problem is solved using the worst-case scenario given the bounded sets of the uncertain parameters. This usually provides an overly conservative solution that does not effectively use the available resources. For the set of statistical approaches, the optimization problem is solved based on the distribution of the uncertain parameters using chance constrains [22]. The chance-constrained approach provides a more accurate solution, but it is generally more difficult to apply because it does not always lead to a convex optimization problem and because of the difficulty of obtaining a closed-form expression for the probability distribution [23]. However, through different types of approximations, the chance-constrained approach has been recently employed for wireless communications, specifically to model the interference constraints in cognitive radio (CR) networks. In [24], Zhang and So analyze the problem of MIMO beamforming of the secondary user (SU) to maximize its throughput while employing chance-constrains to limit the amount of interference to the primary user (PU). In [25], Li *et al.* use the Bernstein approximation method for a chance-constrained resource allocation problem for wireless systems. In [26], Dall'Anese *et al.* develop a power control mechanism for the SU and use chance-constraints for evaluating the aggregate interference at the PU by approximating the sum of interferences as log-normal random variable (RV) using the Fenton-Wilkinson method, and then employ the sequential geometric programming to solve the optimization problem. To the best of our knowledge, chance-constrained optimization approach has not been used for radar and LTE system spectrum sharing.

### B. OUR CONTRIBUTION

In this paper, we are introducing a new spectrum sharing approach for LTE-Unlicensed and radar systems in the 5 GHz band using chance-constrained stochastic optimization. The radar model considered in this development is the ground-based tracking radar as presented in [6]. We choose this radar model to develop a baseline understanding of how LTE can share the spectrum with a well understood radar. Our coexistence model can be easily extended to other radar types in the 5 GHz band. We first analyze the impact of power-controlled LTE base stations on the radar, taking into consideration all the relevant system parameters, including the requirement for the LTE-Unlicensed performance, as given in 3GPP specifications [27]. Then we introduce a novel spectrum sharing approach for the coexistence between radar and LTE-Unlicensed in the same frequency band, based on chance-constrained stochastic optimization. We first analyze the case where there is a single LTE-Unlicensed base station (evolved NodeB or eNodeB) and one radar system. Then we extend our analysis for the aggregate interference, where we formulate an optimization problem to maximize performance of a single eNodeB in the case of multiple eNodeBs sharing the spectrum with a radar system. The rest of the paper is organized as follows: Section II provides the system model. Section III introduces the spectrum sharing algorithm based on the chance-constrained stochastic optimization for the case of a single eNodeB and one radar system. The simulation results for this case are presented in Section IV. Section V provides the spectrum sharing algorithm for the case of multiple eNodeB followed by its numerical analysis in Section VI. We provide our conclusions in Section VII.

## II. SYSTEM MODEL

### A. RADAR TECHNICAL CHARACTERISTICS

The radar under consideration is mono-static with co-located transmit and receive antennas, and with a single target. The radar is transmitting with power $P_0$, so the reflected power from the target at the radar receiver can be modeled as:

$$P_{r_0} = \frac{P_0 G_T G_R \lambda_s^2 \sigma_{RCS}}{(4\pi)^3 L_R} d_{00}^{-4}, \tag{1}$$

where $G_T$ is the radar transmitter antenna gain, $G_R$ is the radar receiver antenna gain, $\lambda_s$ is the signal wavelength, $\sigma_{RCS}$ is the radar cross-section area, $L_R$ is the radar receiver insertion loss, and $d_{00}$ represents the distance between the radar and its target. The antennas used for radars in 5 GHz can be modeled as a function of the off-axis angle ($\theta$) and maximum gain $G_m$. For a high-gain antenna, where ($22 < G_m < 48$ dBi), the antenna gain is modeled as [13]:

$$G(\theta)(dBi) = \begin{cases} G_m - 0.0004 \times 10^{G_m/10}\theta^2 & 0 < |\theta| \le \theta_M \\ 0.75G_m - 7 & \theta_M < |\theta| \le \theta_R \\ 53 - \dfrac{G_m}{2} - 25\log(\theta) & \theta_R < |\theta| \le \theta_B \\ 11 - \dfrac{G_m}{2} & \theta_B < |\theta| \le 180, \end{cases} \tag{2}$$

where the threshold values for the angles are:

$$\begin{aligned} \theta_M &= 50(0.25G + 7)^{0.5}/10^{G/20}, \\ \theta_R &= 250/10^{G/20}, \\ \theta_B &= 48. \end{aligned} \tag{3}$$

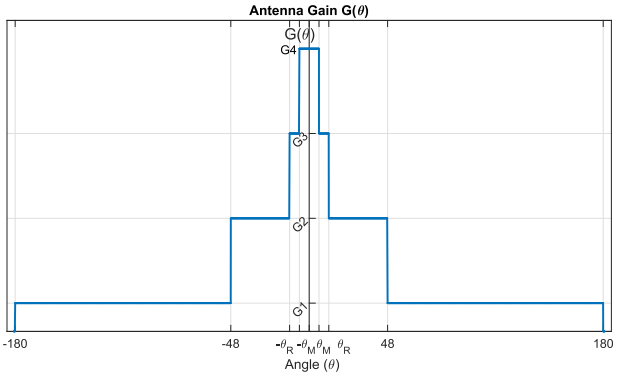


**FIGURE 1.** Radar antenna gain versus angle.

As shown in [20], the antenna pattern can be simplified as shown in Fig. 1 using the following formula:

$$G(\theta)=\begin{cases} G_4 = G_m & 0 < |\theta| \le \theta_M \\ G_3 = 0.75G_m - 7 & \theta_M < |\theta| \le \theta_R \\ G_2 = 53 - \dfrac{G_m}{2} - 25\log(\frac{\theta_B-\theta_R}{2}) & \theta_R < |\theta| \le \theta_B \\ G_1 = 11 - \dfrac{G_m}{2} & \theta_B < |\theta| \le 180. \end{cases} \tag{4}$$

The analysis can be directly extended to a 3D gain pattern, but for the sake of illustration, we limit our analysis to 2D only, with the azimuth angle and without including the effect of the elevation angle. This represents the worst-case scenario, as we are assuming the radar target is always on the ground level. Incorporating the elevation angle will further reduce the effect of the radar on the communications system performance and vice versa.

For the case where there is no interference generated from the communications systems, and for a single received pulse (which is the case for monopulse tracking radars), the signal-to-noise ratio (SNR) for the radar is modeled as:

$$SNR_0 = \frac{P_0 G_T G_R \lambda^2 \sigma_{RCS}}{N_0 (4\pi)^3 L_R} d_{00}^{-4}, \tag{5}$$

where $N_0$ is the noise power at the radar, which is given by:

$$N_0(dBm) = -114 + NF + 10\log(BW), \tag{6}$$

where $NF$ is the noise figure, and $BW$ is the receiver intermediate frequency (IF) bandwidth in MHz [13].

When assuming one single LTE eNodeB transmitting with power level $P_1$ at a distance $d_{10}$ from the radar as shown in Fig. 2, the interference ($\tilde{I}_1$) at the radar becomes:

$$\begin{aligned} \tilde{I}_1(d_{10}) &= \frac{P_1 G_N \tilde{G}_{R1}(\theta_1)\tilde{X}_1}{L_R L_N L_{L_1}(d_{10}) FDR} \\ &= A P_1 C_1 d_{10}^{-\alpha_1} \tilde{G}_{R1}(\theta_1)\tilde{X}_1, \end{aligned} \tag{7}$$

where $\tilde{G}_{R1}(\theta_1)$ is the radar receiver antenna gain in the direction of the eNodeB as a function of angle $\theta_1$ between the radar antenna beam and the eNodeB, and $\tilde{X}_1$ is the shadow fading effect for the path between the eNodeB and the radar. $L_{L_1}$ is the propagation path loss between the eNodeB and the radar as a function of distance $d_{10}$, and it equals $C_1\, d_{10}^{-\alpha_1}$, where $C_1$ is the path loss constant and $\alpha_1$ is the path loss exponent. Parameter $A$ is introduced to simplify the notation, and is given by $A = \frac{G_N}{L_R L_N FDR}$, where $G_N$ is the eNodeB antenna gain, $L_N$ is the eNodeB insertion loss, and $FDR$ is the frequency-dependent rejection at the radar side. For the case of co-channel interference, $FDR$ can be expressed as:

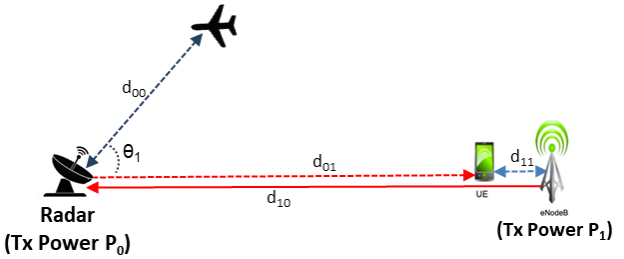


**FIGURE 2.** System model for LTE and radar coexistence.

$$FDR = max\left(1, \frac{BW_{tx}}{BW_{rx}}\right), \tag{8}$$

where $BW_{tx}$ is the emission bandwidth of the undesired transmitted signal, and $BW_{rx}$ is the IF bandwidth of the radar receiver.

It is worth mentioning that, similar to [21], our interference analysis at the radar assumes that the interference comes from the LTE downlink transmission, and that the uplink transmission will have no significant impact to the interference seen at the radar. This claim is justified by two reasons: (i) the LTE-U and LAA (Rel-13) versions of LTE-Unlicensed are defined in the downlink direction only, and (ii) user equipment (UE) operates with much lower transmission power compared to the eNodeB, while time-sharing the channel with it. Since we assume that eNodeB is transmitting with 100% duty cycle, then our analysis represents the worst-case scenario for the interference level at the radar side.

The performance of the radar is dependent on the interference-to-noise ratio (INR). Based on [6], the required INR ($INR_{max}$) to prevent degradation in the radar performance is $-6$ dB. The maximum interference tolerable by the radar $I_{thr}$ is given by:

$$I_{thr}(dB) = N_0 + INR_{max}. \tag{9}$$

### B. LTE-UNLICENSED TECHNICAL CHARACTERISTICS

For the LTE system, and considering the downlink where the eNodeB is transmitting with power level $P_1$, the power received at the receiver device (UE) can be written as

$$P_{r_1} = \frac{P_1 G_N G_U}{L_N L_P \Psi_1} = B P_1, \tag{10}$$

where $G_U$ is the UE receiver gain, $\psi_1$ is a margin to compensate for the large-scale and small-scale fading effect as

typically used for LTE coverage planning [17], and $L_P$ is the propagation loss between the eNodeB and the UE. $B$ is introduced to simplify the notation and equals $\frac{G_N G_U}{L_N L_P \Psi_1}$.

The interference at the UE generated from the radar system is denoted by $\tilde{I}_0$ and is given by:

$$\tilde{I}_0(d_{01}) = \frac{P_0 G_U \tilde{G}_{T1}(\theta_1)\tilde{X}_0}{L_R L_{L_{01}}(d_{01})} = DP_0 C_0 d_{01}^{-\alpha_0} \tilde{G}_{T1}(\theta_1)\tilde{X}_0, \quad (11)$$

where $D$ equals $\frac{G_U}{L_R}$. The radar transmitter antenna gain in the direction of the UE is denoted by $\tilde{G}_{T1}(\theta_1)$, and $\tilde{X}_0$ is the shadow fading effect in the path between the radar and eNodeB. The propagation loss between the radar and the UE is represented by $L_{L_{01}}$ and is a function of the distance between the radar and the UE ($d_{01}$). $L_{L_{01}}$ equals $C_0\ d_{01}^{-\alpha_0}$, where $C_0$ and $\alpha_0$ are the path loss constant and the path loss exponent (for the path from radar to eNodeB), respectively.

LTE-Unlicensed employs the listen-before-talk (LBT) algorithm, which means that the eNodeB senses the spectrum for transmissions from other networks before transmitting to avoid interfering with other LTE or Wi-Fi networks using the same channel. Accordingly, we can assume that there is no interference generated to the UE from neighboring communications networks (no interference from other eNodeB), and the only source of interference is the radar signal. The performance of the LTE link is dependable on the SINR value ($\tilde{\gamma_1}$), which is given by

$$\tilde{\gamma_1} = \frac{BP_1}{DP_0 C_0 d_{01}^{-\alpha_1} \tilde{G}_{T1}(\theta_1)\tilde{X}_0 + N_1}, \quad (12)$$

where $N_1$ is the noise power at the UE.

## III. CHANCE-CONSTRAINED OPTIMIZATION FOR A SINGLE LTE ENODEB SCENARIO

The purpose of the optimization problem is to determine the maximum power level the eNodeB can use based on its relative distance to the radar system. Determining the relative distance to the radar can be done centrally through a database, where the eNodeB registers its location before accessing the channel, and the central database solves the optimization problem and determines the maximum transmitted power for the eNodeB. Alternately, it can be done at the eNodeB where it uses a learning algorithm to measure the interference generated by the radar to estimate the relative distance to the radar. The minimum performance for the LTE system will be given at the cell edge, where we assume that the UE is in the same direction of the radar, so this represents the worst-case performance for any UE served by that eNodeB. So the value taken by the RV $\tilde{G}_{R1}(\theta_1)$ at the angle ($\theta_1$) is equal to the one of $\tilde{G}_{T1}(\theta_1)$, and $d_{10} = d_{01} - d_{11}$, where $d_{11}$ is the cell radius coverage.

### A. PROBLEM FORMULATION

The optimization problem is formulated to maximize the power $P_1$ of the eNodeB while satisfying the condition of not creating unacceptable interference at the radar side, and delivering an acceptable performance requirement for the UE. So the chance-constrained stochastic optimization problem is expressed mathematically as follows:

$$\begin{aligned} &\text{maximize } P_1 \\ &\text{subject to } \Pr(\tilde{I}_1 \le I_{thr}) \ge \beta_0 \\ &\qquad \Pr(\tilde{\gamma_1} \ge \gamma_L) \ge \beta_1 \\ &\qquad P_1 \ge 0 \\ &\qquad P_1 \le P_{L,max} \end{aligned} \quad (13)$$

where $\gamma_L$ is the SINR threshold at the UE, $\beta_0$ is the confidence level for achieving the minimum requirement for radar performance, and $\beta_1$ is the confidence level for achieving the minimum requirement for LTE performance. The analysis boils down to a simple rule, the eNodeB transmits with the maximum power if no interference is produced at the radar side or transmits with the power level that keeps the interference at the radar side below a certain threshold level and, at the same time, delivers the minimum required SNR at the UE. If these two conditions cannot be met, the eNodeB does not transmit at all.

### B. ANALYSIS

Considering the first constraint in the optimization problem (13), we can note from (7) that $\tilde{I}_1$ is a function of two RVs, $\tilde{G}_{R1}(\theta_1)$ and $\tilde{X}_1$. $\tilde{G}_{R1}(\theta_1)$ is treated as a RV due to the uncertainty of the radar antenna direction, which is function of the target location. A practical radar points the main antenna beam in the direction of the target, so the antenna gain in the direction of the eNodeB will be changing as well. Accordingly, the interference between the radar and the eNodeB will change based on changing the radar antenna direction. So let us define a RV $\tilde{Z} = \tilde{G}_{R1}(\theta_1)\tilde{X}_1$, so the constraint equation can be re-formulated as

$$\begin{aligned} &\Pr\big(AP_1 C_1 d_{10}^{-\alpha_1} \tilde{Z} \le I_{thr}\big) \ge \beta_0 \\ &\Pr\big(\tilde{Z} \le \frac{I_{thr}}{AP_1 C_1 d_{10}^{-\alpha_1}}\big) \ge \beta_0 \\ &F_Z\big(\frac{I_{thr}}{AP_1 C_1 d_{10}^{-\alpha_1}}\big) \ge \beta_0 \end{aligned} \quad (14)$$

where $F_Z()$ is the cumulative distribution function (CDF) for $\tilde{Z}_1$. To obtain $F_{Z_1}()$, let us first consider the two factors of $\tilde{Z}_1$.

For $\tilde{G}_{R1}(\theta_1)$, since we are dealing with a tracking radar, where the target can be at any angle from the radar, then $\theta_1$ can be modeled as circular uniform random variable in [0 - 360] degrees. Based on this, and based on the radar gain pattern given in (4), the probability density function (PDF) for the radar antenna gain in direction of the eNodeB $f_{G_{R1}}$

then becomes

$$f_{G_{R1}}(g) = \begin{cases} \frac{180-\theta_B}{180}\delta(g-G_1) = w_1 G_1 & g = G_1 \\ \frac{\theta_B-\theta_R}{180}\delta(g-G_2) = w_2 G_2 & g = G_2 \\ \frac{\theta_R-\theta_M}{180}\delta(g-G_3) = w_3 G_3 & g = G_3 \\ \frac{\theta_M}{180}\delta(g-G_4) \quad = w_4 G_4 & g = G_4 \\ 0 & Otherwise \end{cases} \quad (15)$$

where $g$ is the random variable represents the radar antenna gain and $\delta(.)$ is the Dirac delta function.

As considered in several previous research works, the shadow fading can be modeled by a log-normal distribution with zero mean and standard deviation $\sigma_1$, the PDF of $\tilde{X}_1$ is obtained as [28]

$$f_{X_1}(x) = \frac{1}{x\sqrt{2\pi}\sigma_1}\exp[-\frac{\ln(x)^2}{2{\sigma_1}^2}] \quad 0 < x < \infty. \quad (16)$$

Since both $\tilde{G}_{R1}(\theta_1)$ and $\tilde{X}_1$ are uncorrelated, $F_{Z_1}$ can be expressed by [29]

$$\begin{aligned} F_{Z_1}(z) &= \int_{g=0}^{g=G_m}\int_{x=0}^{x=\frac{z}{g}} f_{G_{R1}}(g) f_{X_1}(x) dg dx \\ &= \int_{g=0}^{g=G_m} f_{G_{R1}}(g)[\frac{1}{2} + \frac{1}{2}erf\big(\frac{ln(z/g)}{\sqrt{2}\sigma_1}\big)]\, dg \\ &= \frac{1}{2}\sum_{i=1}^{4} w_i + \frac{1}{2}\sum_{i=1}^{4} w_i\, erf\big(\frac{ln(z/g)}{\sqrt{2}\sigma_1}\big) \\ &= \frac{1}{2} + \frac{1}{2}\sum_{i=1}^{4} w_i\, erf\big(\frac{ln(z/G_i)}{\sqrt{2}\sigma_1}\big) \end{aligned} \quad (17)$$

where $G_m$ is the maximum radar antenna gain as in (4), $G_i$ is the radar antenna gain with index $i$ as shown in (15), and erf(.) is the error function.

So the first constraint can be expressed deterministically as

$$\begin{aligned} &\frac{1}{2}+\frac{1}{2}\sum_{i=1}^{4} w_i\, erf\big(\frac{ln(\frac{I_{thr}}{AP_1C_1(d_{10})^{-\alpha_1}})-\ln(G_i))}{\sqrt{2}\sigma_1}\big) \geq \beta_0 \\ &or \\ &\sum_{i=1}^{4} w_i\, erf\big(\frac{ln(\frac{I_{thr}}{AP_1C_1(d_{10})^{-\alpha_1}})-\ln(G_i)}{\sqrt{2}\sigma_1}\big) \geq 2(\beta_0-0.5) \end{aligned} \quad (18)$$

For the second constraint in the optimization problem (13), we can note from (12) that $\tilde{\gamma}_0$ is also a function of two random variables (RVs), $\tilde{G}_{T1}(\theta_1)$ and $\tilde{X}_0$. So by defining a RV $\tilde{Z}_0 = \tilde{G}_{T1}(\theta_1)\tilde{X}_0$, the constraint equation can be re-formulated as

$$\begin{aligned} \Pr\big(\frac{BP_1}{DP_0C_0(d_{01})^{-\alpha_1}\tilde{G}_{T1}(\theta_1)\tilde{X}_0 + N_1} \geq \gamma_L\big) &\geq \beta_1 \\ \Pr\big(\frac{BP_1 - N_1\gamma_L}{\gamma_L DP_0C_0(d_{01})^{-\alpha_1}} \geq \tilde{G}_{T1}(\theta_1)\tilde{X}_0\big) &\geq \beta_1 \\ F_{Z_0}\big(\frac{BP_1 - N_1\gamma_L}{\gamma_L DP_0C_0(d_{01})^{-\alpha_1}}\big) &\geq \beta_1. \end{aligned} \quad (19)$$

The RV $\tilde{X}_0$ is also modeled by a log-normal distribution with zero mean and standard deviation $\sigma_0$ and the RV $\tilde{G}_{T1}(\theta_1)$ has the same PDF of $\tilde{G}_{R1}(\theta_1)$. Accordingly, and following the same approach used for the first constraint, the second constraint of (13) can be written as

$$\sum_{i=1}^{4} w_i\, erf\big(\frac{ln(\frac{BP_1-N_1\gamma_L}{\gamma_L DP_0C_0(d_{01})^{-\alpha_1}}) - \ln(G_i))}{\sqrt{2}\sigma_0}\big) \geq 2(\beta_1-0.5) \quad (20)$$

The optimization problem (13) can then be reformulated as

$$\begin{aligned} \text{maximize} \quad & P_1 \\ \text{subject to:} \quad & \sum_{i=1}^{4} w_i\, erf \\ & \times \big(\frac{ln(\frac{I_{thr}}{AP_1C_1(d_{10})^{-\alpha_1}} - \ln(G_i))}{\sqrt{2}\sigma_1}\big) \geq 2(\beta_0-0.5) \\ & \sum_{i=1}^{4} w_i\, erf \\ & \times \big(\frac{ln(\frac{BP_1-N_1\gamma_L}{\gamma_L DP_0C_0(d_{01})^{-\alpha_1}} - \ln(G_i))}{\sqrt{2}\sigma_0}\big) \geq 2(\beta_1-0.5) \\ & P_1 \geq 0 \\ & P_1 \leq P_{L,max} \end{aligned} \quad (21)$$

As shown in the final formulation of the proposed chance-constraint (CC) optimization problem in (21), the first constraint represent the upper limit for the eNodeB transmission power ($P_1$) in order to limit the interference level at the radar side (as the first constraint requires $P_1$ to be decreased). The second constraint represents the lower limit for ($P_1$) in order to ensure that the SINR at the UE will be higher than a given threshold value $\gamma_L$ (as the second constraint requires $P_1$ to be increased).

## IV. NUMERICAL RESULTS FOR SINGLE LTE ENODEB

The detailed parameters for the radar system are given Table 1, where the stationary Radar 5 was chosen as an example of a tracking radar in the 5 GHz; the proposed algorithm can be extended to any different stationary tracking radar within this band. The parameters for the LTE system and the channel are given in Table 2. As previously mentioned, the required INR to prevent degradation of the radar performance is $-6$ dB, which corresponds to $I_{th} = -105.97\ dBm$. For the LTE system, and as per the 3GPP specifications in [27], the minimum SNR required for the UE to decode the control and data channel ($\gamma_L$) in TDD mode is 1.2 dB. The confidence levels of the second constraint ($\beta_1$) is chosen to be 95%, while we provide the results for three different values of ($\beta_0 = 95\%,\ 95\%,\ and\ 99\%$). The cell radius of the LTE-Unlicensed was chosen to be 50 m, which is a typical value for small-cell coverage at the 5 GHz band.

The propagation path model we use in this study is the well-known Longley-Rice model (LR), which is based on

**TABLE 1. Radar simulation parameters.**

| Parameter Name | Value |
|---|---|
| Radar Type | Radar 5 |
| Radar Platform | Ground-Based |
| Frequency | 5.50 GHz |
| Radar Transmit Power $P_0$ | 165 KW |
| Radar Maximum Gain | 42 dBi |
| Radar Normalized Antenna Gain | G4=1<br>G3 = $1.78 \times 10^{-2}$<br>G2 = $3.35 \times 10^{-4}$<br>G3 = $6.3 \times 10^{-6}$ |
| Radar Antenna Angle Threshold | $\theta_M = 1.66^o$<br>$\theta_R = 1.99^o$<br>$\theta_B = 48^o$ |
| Radar Insertion Losses $L_R$ | 2 dB |
| Radar IF 3-dB BW | 8 MHz |
| Radar $FDR_0$ | 2.5 |
| Radar Noise Figure $NF$ | 5 dB |
| Radar Noise Power $N_0$ | -99.97 dBm |
| Radar Maximum Tolerable INR | -6 dB |
| Aggregate Interference Threshold | -105.97 dBm |

**TABLE 2. LTE and channel simulation parameters.**

| Parameter Name | Value |
|---|---|
| eNodeB Maximum Transmit Power | 1000 mWatt |
| eNodeB Antenna Type | Omni |
| eNodeB Antenna Gain | 6 dBi |
| eNodeB Insertion Losses $L_N$ | 2 dB |
| LTE BW | 20 MHz |
| eNodeB Noise Floor $N_1$ | -95.99 dBm |
| UE Antenna Gain | 0 dBi |
| eNodeB Noise Figure $NF$ | 9 dB |
| UE Noise Power | -91.99 dBm |
| Margin to compensate for large and small scale fading between eNodeB and UE ($\psi_1$) | 6 dB |
| $\gamma_L$ | 1.2 dB |
| Standard deviation of shadow fading ($\sigma_0$ and $\sigma_1$) | 6 dB |

field measurements. There is no-closed form expression for this model, but an exponential curve fitting was performed in [19] and the propagation path loss as a function of the distance between a transmitter and a receiver ($d$, expressed in meters) is given by

$$L_L = 259\, d^{-3.97} \tag{22}$$

The large-scale and small-scale fading effects in the channel between the eNodeB and the UE are compensated by a margin ($\psi_1$) equal to 6 dB to ensure 95% edge coverage reliability.

To evaluate the performance of the chance-constraint (CC) optimization algorithm, we analyze the bounds of the protection distance currently specified by the regulations. The current regulations for accessing the 5 GHz spectrum require implementing the DFS technique. For us to determine the distance at which the eNodeB receives a radar signal above the DFS threshold, and using a 95% margin for the shadow fading effect, we need to use the boundaries for an eNodeB receiving in the direction of the radar main-beam (using $G_{R1,max} = G4$) and for the case when receiving in the direction of the back-lobe of the radar antenna (using $G_{R1,min} = G1$). The protection distance using $G_{R1,max}$ is 469.9 km, while using $G_{R1,min}$, the protection distance is 23.06 km.

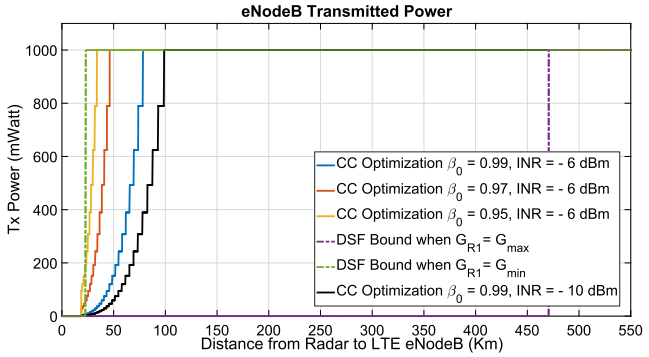


**FIGURE 3. Comparison of the proposed CC optimization algorithm to the boundaries for acceptably radar and UE performance for a single-cell scenario.**

The power levels available for the eNodeB are discrete, as the eNodeB is only able to change its transmission power with a 1 dB step size (based on the hardware limitations), so we use the exhaustive search (brute-force search) to solve the optimization problem. We solve the optimization problem for the power range from 30 dBm (maximum eNodeB transmit power in the 5 GHz based on the 3GPP specifications) to $-20$ dBm. Fig. 3 provides a comparison of the proposed CC-optimization algorithm to the DFS boundaries as a function of the distances between the radar and the eNodeB for three different values of $\beta_0$. Using a $\beta_0 = 99\%$, the eNodeB will have to reduce its transmission power when its relative distance to the radar is around 78.3 km, and the maximum allowable Tx power will be decreased (in steps of 1 dB) if the distance between eNodeB and radar is decreased. The minimum protection distance between the two systems is 18.6 km (the eNodeB Tx power is 11 dBm in this case); this is the distance below which the SINR performance at the UE will start dropping below the acceptable level. Using $\beta_0 = 97\%$, the first constraint is relaxed, so the eNodeB is allowed to use the maximum transmit power level at a distance of 46.2 km away from the radar. When relaxing the first constraint even more and using the confidence level of $\beta_0 = 95\%$, the eNodeB is allowed to use the maximum transmit power level at a distance of 33.8 km away, below which the maximum transmission power will have to be decreased until a distance of 18.6 km as well, as this value is limited by the SINR performance at the UE. At this distance, the transmitted power of the eNodeB is too low, and the interference level from the radar at the UE is too high, so the resulting SINR is below the threshold level. In other words, the proposed algorithm estimates a reduced transmission power for the eNodeB when the relative distance to the radar is decreased. Accordingly, the protection distance between the radar and the eNodeB will be decreased more than the one specified by the regulations, thanks to smart power control. Note that these results could be tied into the scheduler to reduce power via increased bandwidth allocation to always pressure the link.

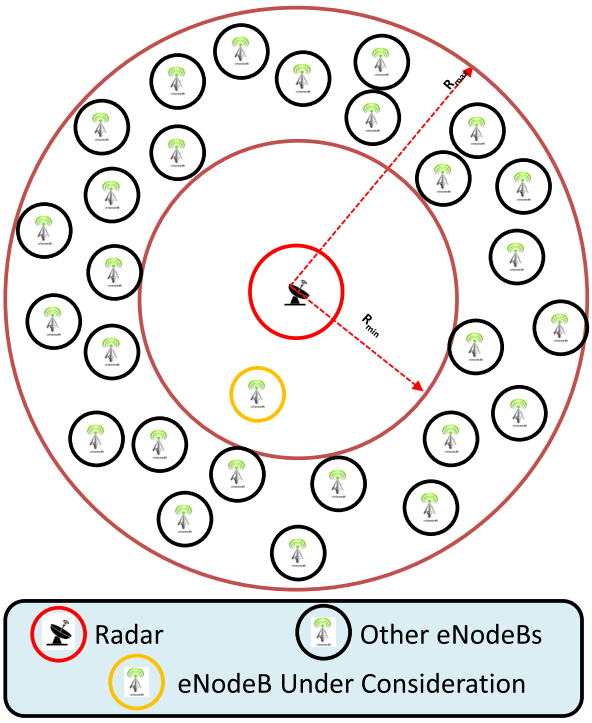


**FIGURE 4.** Multiple eNodeBs interference scenario.

The radar sensitivity is captured in the analysis by the INR. According to [6], it was suggested to use an INR of $-10$ dB for the radionavigation service and meteorological1 radars due to the safety-of-life function of these types of radars. We have evaluated the performance for the proposed CC optimization algorithm for the case when INR equals $-10$ dB (which is equivalent to an aggregate interference threshold level of $-109.97$ dBm) and when the confidence level is equal to $\beta_0 = 99\%$. As shown in Fig. 3, the eNodeB is allowed to transmit with the maximum power up to a distance of 100 km, which is around 22 km increase in the protection distance compared to the case when the INR equals $-6$ dB.

## V. CHANCE-CONSTRAINED OPTIMIZATION FOR A SINGLE ENODEB IN A MULTIPLE CELLS SCENARIO

### A. PROBLEM FORMULATION

In this section, we extend the previous scenario to a more generalized one, where the eNodeB is surrounded by other multiple cells. In this scenario, the Tx power of a single eNodeB is to be maximized while satisfying the condition that the aggregate interference generated from all eNodeBs ($\tilde{I}_t$) is less than the threshold level for the maximum tolerable interference at the radar while delivering the adequate performance requirement for the UE served by that eNodeB. Fig. 4 shows the scenario for multiple eNodeBs sharing the spectrum with a radar. As seen in the previous section, even for a single eNodeB, there is a minimum distance around the radar ($R_{min}$) where there is no feasible solution to the optimization problem, and we are considering the eNodeBs that can affect the radar performance if they transmit within a distance range of ($R_{max}$). The aggregate interference generated from all eNodeBs denoted by ($\tilde{I}_t$), which is the summation of interference generated from all eNodeBs ($\sum_{k=1}^{K} \tilde{I}_k$), where $K$ is the total number of eNodeBs in the geographical area bounded by $R_{min}$ and $R_{max}$. Without loss of generality, we assume we are maximizing the power level $P_1$, while the transmitted power of all other eNodeBs is denoted by $P_k$, where $k = 2, 3, \ldots, K$. So the proposed CC optimization problem is formulated as:

$$\begin{aligned} &\text{maximize } P_1 \\ &\text{subject to } \Pr(\tilde{I}_t = \sum_{k=1}^{K} \tilde{I}_k \leq I_{thr}) \geq \beta_0 \\ &\qquad \Pr(\tilde{\gamma}_1 \geq \gamma_L) \geq \beta_1 \\ &\qquad P_1 \geq 0 \\ &\qquad P_1 \leq P_{L,max} \end{aligned} \tag{23}$$

### B. ANALYSIS

The second constraint of the optimization problem (23) is similar to the single-cell scenario, so we need to find a closed-form expression for the first constraint. Since the interference generated from every other eNodeB ($\tilde{I}_k$, $\forall k = 2, 3, \ldots, K$) is dependent on the distance between an arbitrary eNodeB ($k$) (with unknown location) to the radar, we need to handle that distance $\tilde{d}_{k0}$ as a RV. We assume that the eNodeBs are uniformly distributed around the radar. So the PDF for $\tilde{d}_{k0}$ and is given by:

$$f_D(d_{k0}) = \frac{2d_{k0}}{R_{max}^2 - R_{min}^2} \tag{24}$$

So the first constraint in (23) can be formulated as:

$$\Pr(\sum_{k=1}^{K} A P_k C_k \tilde{d}_{k0}^{-\alpha_k} \tilde{G}_{Rk}(\theta_1) \tilde{X}_k \leq I_{thr}) \geq \beta_0. \tag{25}$$

We can assume that the path loss constant and the path loss exponent are the same for all eNodeBs, so $C_k = C_1$ and $\alpha_k = \alpha$, $\forall k = 1, 2, \ldots K$. Also since we assume that the eNodeBs are uniformly distributed in a circle area around the radar, and based on the law of large numbers, the antenna gain of the radar towards each eNodeB can be modeled as the average radar antenna gain $G_{R,avg}$ which is given by:

$$G_{R,avg} = \sum_{i=1}^{4} w_i \, G_i. \tag{26}$$

So the first constraint in (25) can be written as:

$$\begin{aligned} &\Pr(\sum_{k=1}^{K} A P_k C_1 \tilde{d}_{k0}^{-\alpha} G_{R,avg} \tilde{X}_k \leq I_{thr}) \geq \beta_0 \\ &\textit{or} \\ &\Pr(\sum_{k=1}^{K} P_k \tilde{d}_{k0}^{-\alpha} \tilde{X}_k \leq \frac{I_{thr}}{A C_1 G_{R,avg}}) \geq \beta_0. \end{aligned} \tag{27}$$

It is clear from (27) that the aggregate interference is the summation of log-normal RVs. There is no closed form

for this summation, but it is well-known that this summation can be approximated by another log-normal RV (let us denote it by $\tilde{Y}_t$), with a mean of $\mu_t$ and variance of $\sigma_t^2$. There are several methods that are commonly used for such approximations that use a cumulant-matching technique, such as the Fenton-Wilkinson and Schwartz-Yeh methods. Fenton-Wilkinson is more suitable for our purpose as it is more computationally efficient and provides good approximation at the tail region of the distribution, which is our main concern [26]. Accordingly, the first constraint can be reformulated as:

$$\begin{aligned}&\Pr(\tilde{Y}_t \le \frac{I_{thr}}{AC_1G_{R,avg}}) \ge \beta_0\\ &or\\ &\Pr(\tilde{Y}_t > \frac{I_{thr}}{AC_1G_{R,avg}}) \le (1-\beta_0).\end{aligned} \tag{28}$$

As shown in [26], this can be given by:

$$\Pr(\tilde{Y}_t \ge \frac{I_{thr}}{AC_1G_{R,avg}}) = Q\Big(\frac{ln(\frac{I_{thr}}{AC_1G_{R,avg}}) - \mu_t}{\sigma_t}\Big) \le (1-\beta_0)$$

*Accordinly*

$$\mu_t + Q^{-1}(1-\beta_0)\sigma_t \le ln(\frac{I_{thr}}{AC_1G_{R,avg}}), \tag{29}$$

where Q(.) is the Q-function.

So the optimization problem in (23) can be formulated as:

$$\begin{aligned}&\text{maximize } P_1\\ &\text{subject to } \mu_t + Q^{-1}(1-\beta_0)\sigma_t \le ln(\frac{I_{thr}}{AC_1G_{R,avg}})\\ &\sum_{i=1}^{4} w_i\, erf\\ &\times \Big(\frac{ln(\frac{BP_1 - N_1\gamma_L}{\gamma_L DP_0C_0(d_{01})^{-\alpha_1}} - \ln(G_i))}{\sqrt{2}\sigma_0}\Big) \ge 2(\beta_1 - 0.5)\\ &P_1 \ge 0\\ &P_1 \le P_{L,max}\end{aligned} \tag{30}$$

So it is required that we get the mean ($\mu_t$) and the standard deviation ($\sigma_t$) of the log-normal RV $\tilde{Y}_t$. Based on the Fenton-Wilkinson approximation, it was shown in [30], that for the case of the summation of $\sum_k A_k\tilde{X}_k$, where $A_k$'s are positive independent random variables, the mean $\mu_t$ and variance of $\sigma_t^2$, can be written as [31]

$$\begin{aligned}\mu_t &= \ln(\frac{m^2}{\sqrt{m^2+s^2}}),\\ \sigma_t^2 &= \ln(\frac{s^2}{m^2}+1),\end{aligned} \tag{31}$$

where

$$\begin{aligned}m &= \sum_{k=1}^{K} P_k E[\tilde{d}_{k0}^{-\alpha}]E[\tilde{X}_k],\\ s^2 &= \sum_{k=1}^{K}\sum_{j=1}^{K} P_kP_j cov(\tilde{X}_k\tilde{d}_{k0}^{-\alpha}, \tilde{X}_j\tilde{d}_{j0}^{-\alpha_j}),\end{aligned} \tag{32}$$

where $cov(X,Y)$ is the covariance between the two random variable $X$ and $Y$.

Since we assume that the shadow fading effects $\tilde{X}_k$ are independent and identically distributed (i.i.d) [32], $E[\tilde{X}_k] = E[\tilde{X}] = \exp(\lambda^2\frac{\sigma^2}{2})\ \forall k = 1, 2, \ldots, K$, where $\lambda = \frac{ln10}{10}$. Also, $E[\tilde{X}^2] = \exp((2\lambda^2\sigma^2)$. Based on the PDF of $(\tilde{d}_{k0})$ given in (24), the $E[\tilde{d}_{k0}^{-\alpha}]$ and $E[\tilde{d}_{k0}^{-2\alpha}]$ can be calculated as

$$\begin{aligned}E[\tilde{d}_{k0}^{-\alpha}] &= \frac{2(R_{max}^{2-\alpha} - R_{min}^{2-\alpha})}{(2-\alpha)(R_{max}^2 - R_{min}^2)} \quad \forall k = 2, 3, \ldots, K\\ E[\tilde{d}_{k0}^{-2\alpha}] &= \frac{(R_{max}^{2-2\alpha} - R_{min}^{2-2\alpha})}{(1-\alpha)(R_{max}^2 - R_{min}^2)} \quad \forall k = 2, 3, \ldots, K\end{aligned} \tag{33}$$

Since we are interested in identifying the power $P_1$ for an eNodeB at distance ($d_{10}$), we can calculate $m$ in (32) as

$$\begin{aligned}m &= P_1 d_{10}^{-\alpha}E[\tilde{X}] + \sum_{k=2}^{K} P_k E[\tilde{d}_{k0}^{-\alpha}]E[\tilde{X}]\\ &= P_1 d_{10}^{-\alpha}E[\tilde{X}] + E[\tilde{X}]\,\frac{2(R_{max}^{-\alpha} - R_{min}^{-\alpha})}{(2-2\alpha)R_{max}^2 - R_{min}^2}\sum_{k=2}^{K} P_k\end{aligned} \tag{34}$$

If all other eNodeBs are employing DFS algorithm, then we can assume that all of these eNodeBs transmit all the time with the maximum power denoted by $P_{n,max}$. Note that we assume that each eNodeB will be transmitting in the downlink all the time with the maximum power. In case of the eNodeB dividing the TDD frame between downlink and uplink, the transmitted power of the UE will be much less than that of the eNodeB, so we are optimizing for the worst-case scenario. Accordinly:

$$m = P_1 d_{10}^{-\alpha}E[\tilde{X}] + (K-1)P_{n,max}E[\tilde{X}]\frac{2(R_{max}^{-\alpha} - R_{min}^{-\alpha})}{(2-\alpha)R_{max}^2 - R_{min}^2}. \tag{35}$$

For $s^2$ in (32), it can be calculated as [31]

$$\begin{aligned}s^2 &= \sum_{k=1}^{K}\sum_{j=1}^{K} P_kP_j cov(\tilde{X}_k\tilde{d}_{k0}^{-\alpha}, \tilde{X}_j\tilde{d}_{j0}^{-\alpha})\\ &= \sum_{k=1}^{K} P_k^2\, var\{\tilde{X}_k\tilde{d}_{k0}^{-\alpha}\} + \sum_{k=1}^{K}\sum_{j=1, i\ne j}^{K} P_kP_j\, cov(\tilde{X}_k\tilde{d}_{k0}^{-\alpha}, \tilde{X}_j\tilde{d}_{j0}^{-\alpha})\\ &= E[\tilde{X}^2]\sum_{k=1}^{K} P_k^2 E[\tilde{d}_{k0}^{-2\alpha}] - E^2[\tilde{X}]\{\sum_{k=1}^{K} P_k E[\tilde{d}_{k0}^{-\alpha_k}]\}^2\\ &\quad + E^2[\tilde{X}]\sum_{k=1}^{K}\sum_{j=1, j\ne k}^{K} P_kP_j\, E[\tilde{d}_{k0}^{-\alpha}, \tilde{d}_{j0}^{-\alpha}]\\ &= S1 - S2 + S3,\end{aligned} \tag{36}$$

where $S1$, $S2$, and $S3$ are introduced to simplify the notation and to analyze each term on the summation separately. $S1$ can be given by:

$$\begin{aligned}S1 &= E[\tilde{X}^2]\sum_{k=1}^{K} P_k^2 E[\tilde{d}_{k0}^{-2\alpha}]\\ &= E[\tilde{X}^2]P_1^2 d_{10}^{-2\alpha} + E[\tilde{X}^2](K-1)P_{n,max}^2 E[\tilde{d}_{k0}^{-2\alpha}].\end{aligned} \tag{37}$$

For $S2$, we obtain

$$S2 = E^2[\tilde{X}]\{\sum_{k=1}^{K} P_k E[\tilde{d}_{k0}^{-\alpha_k}]\}^2$$
$$= E^2[\tilde{X}]\{P_1 d_{10}^{-\alpha} + (K-1)P_{n,max}E[\tilde{d}_{k0}^{-\alpha}]\}^2. \quad (38)$$

For $S3$, since it is not possible to get a closed-form expression for $E[\tilde{d}_{k0}^{-\alpha}, \tilde{d}_{j0}^{-\alpha}]$, we will use the upper bound for it using the Cauchy-Schwartz inequality:

$$E[\tilde{d}_{k0}^{-\alpha}, \tilde{d}_{j0}^{-\alpha}] \leq \sqrt{E[\tilde{d}_{k0}^{-2\alpha}]E[\tilde{d}_{j0}^{-2\alpha}]}, \quad (39)$$

so the upper bound for $S3$ is

$$S3 = E^2[\tilde{X}]\sum_{k=1}^{K}\sum_{j=1,j\neq k}^{K} P_k P_j E[\tilde{d}_{k0}^{-\alpha}, \tilde{d}_{j0}^{-\alpha}]$$
$$\leq E^2[\tilde{X}]\sum_{k=1}^{K}\sum_{j=1,j\neq k}^{K} P_k P_j \sqrt{E[\tilde{d}_{k0}^{-2\alpha}]E[\tilde{d}_{j0}^{-2\alpha}]}$$
$$\leq E^2[\tilde{X}]\{2(K-1)P_{n,max}P_1 d_{10}^{-\alpha}E[\tilde{d}_{k0}^{-\alpha}]$$
$$+ (K-1)(K-2)P_{n,max}^2 E[\tilde{d}_{k0}^{-2\alpha}]\} \quad (40)$$

So accordingly, $s^2$ written as

$$s^2 = E[\tilde{X^2}]P_1^2 d_{10}^{-2\alpha} + E[\tilde{X^2}](K-1)P_{n,max}^2 E[\tilde{d}_{k0}^{-2\alpha}]$$
$$- E^2[\tilde{X}]\{P_1 d_{10}^{-\alpha} + (K-1)P_{n,max}E[\tilde{d}_{k0}^{-\alpha}]\}^2$$
$$+ E^2[\tilde{X}]\{2(K-1)P_{n,max}P_1 d_{10}^{-\alpha}E[\tilde{d}_{k0}^{-\alpha}]$$
$$+ (K-1)(K-2)P_{n,max}^2 E[\tilde{d}_{k0}^{-2\alpha}]\} \quad (41)$$

After simplifications for $s^2$, we have:

$$s^2 = \{E[\tilde{X^2}] - E^2[\tilde{X}]\}P_1^2 d_{10}^{-2\alpha}$$
$$+ \{(K-1)E[\tilde{X^2}]E[\tilde{d}_{k0}^{-2\alpha}]$$
$$- (K-1)^2 E^2[\tilde{X}]E^2[\tilde{d}_{k0}^{-\alpha}]$$
$$+ (K-1)(K-2)E^2[\tilde{X}]E[\tilde{d}_{k0}^{-2\alpha}]\}P_{n,max}^2 \quad (42)$$

So subtitling the calculated values for $m$ and $s^2$ from (42) and (35) in (31), we can calculate the mean ($\mu_t$) and standard deviation ($\sqrt{\sigma_t^2}$) required to solve the optimization problem for multiple cells in (30).

## VI. NUMERICAL RESULTS FOR MULTIPLE LTE ENODEBS SCENARIO

Not only the performance of the proposed CC optimization algorithm is affected by the confidence level at the radar side ($\beta_0$), but also it is affected by the total aggregate interference level from all other eNodeBs. The total aggregate interference is a function of the number of eNodeBs ($N$) and the value of ($R_{min}$), which indicates the minimum allowable distance at which the an eNodeB is allowed to transmit. We analyze the effect of each parameter separately. In all cases, the performance of the proposed CC optimization algorithm is compared to the boundaries of the DFS algorithm similar to the case of a single-eNodeB scenario. Also we consider that all eNodeBs are within range of ($R_{max} = 600$ km).

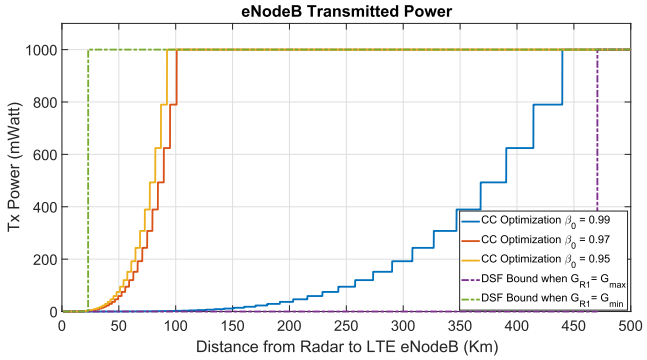


**FIGURE 5. Comparison of the proposed chance-constrained optimization algorithm to the DFS boundaries for multiple cells scenario using different values of $\beta_0$.**

### A. EFFECT OF $\beta_0$

We compare the effect of $\beta_0$ on the performance of the proposed algorithm using ($R_{min} = 469.9$ km), which is the DFS limit assuming the maximum radar antenna gain, and assuming total number of eNodeBs ($K = 10,000$). Fig. 5 shows a comparison for the effect of $\beta_0$ ranging from 95% to 99%. The results of the proposed algorithm with $\beta_0$ equal to 95% and 97% are close to each other, where the distances at which the eNodeB needs to reduce its power from the maximum level is close to each other. With the case of $\beta_0 =$ 99% and for that large number of other eNodeBs, the proposed algorithm requires the eNodeB to start decreasing its transmit power gradually at a distance of 439.7 km. This because at high confidence level, the aggregate interference is dominated by the ones received from other eNodeBs. While when relaxing the confidence level, the dominant term in the summation of the aggregate interference is the one received for the single eNodeB applying the CC optimization algorithm.

### B. EFFECT OF K

The proposed algorithm ensures that the aggregate interference from the radar must be below the INR threshold. So the total number of eNodeBs affect the performance of the algorithm, as the eNodeB will not be able to transmit if the aggregate interference from other eNodeBs already exceeding the threshold. Using ($R_{min} = 469.9$ km) and ($\beta_0 = 95\%$), Fig. 6 provides a comparison for the proposed algorithm for different number of the total eNodeBs. When the number of total eNodeBs increases, the eNodeB applying the proposed algorithm is required to reduce its transmit power level from the maximum at a larger distance from the radar. However, it is clear that the effect of increasing $K$ is small when $K$ is within the smaller range (e.g, from 100 to 1,000 ), because the level of aggregate interference to the eNodeBs has minimal effect when $K$ is small as the dominant effect on the CC optimization algorithm is the distance between that eNodeB applying the CC optimization algorithm and the radar. With large values of $K$, the performance is dominated by the aggregate interference at the radar from other eNodeBs.

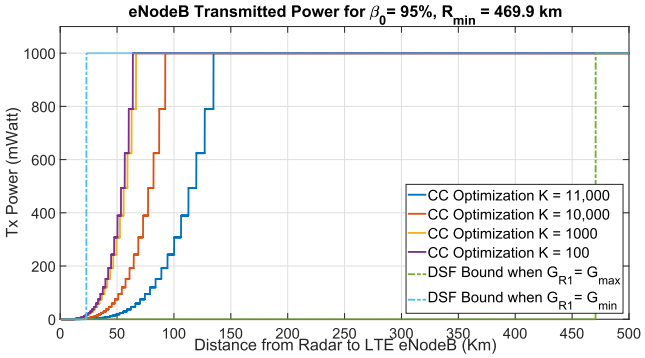


**FIGURE 6.** Chance-constrained optimization algorithm for different values of multiple cells $K$.

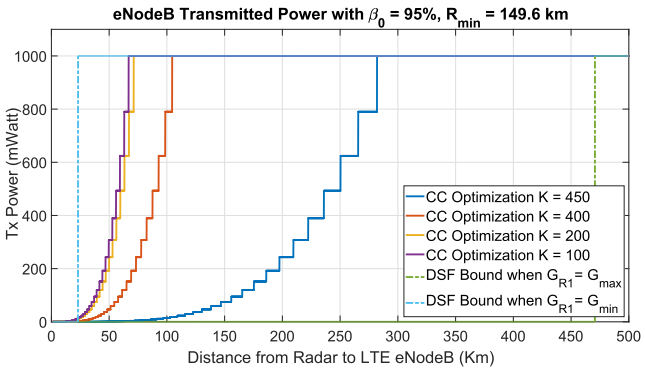


**FIGURE 7.** Chance-constrained optimization algorithm for a different values of $K$ using $R_{min}$ = 149.9 km.

### C. EFFECT OF $R_{MIN}$

In the previous analysis, we limited the number of total eNodeBs to the ones that can detect the DFS threshold value assuming the radar is transmitting with the maximum antenna gain, which is quite optimistic approach for the single eNodeB employing CC optimization algorithm. A more practical approach is to calculate $R_{min}$ assuming all eNodeBs will detect the DFS threshold using the average antenna gain of the radar. Fig. 7 shows a comparison for the performance of the CC optimization algorithm at different values of $K$ using $R_{min}$ = 149.9 km and using $\beta_0 = 95\%$. The maximum number of $K$ that can allow the eNodeB to apply the CC optimization algorithm will be in the range of 450 eNodeBs. This number will greatly increase if we take into consideration the 30 minutes non-occupancy period mandated by the DFS regulations. Because any eNodeB that detects a radar signal above the DFS detection threshold will not be allowed to transmit for 30 minutes, this allows to increase the total number of other eNodeBs that can accommodate a single eNodeB to deploy the CC optimization algorithm.

Fig. 8 shows the performance of the proposed CC optimization algorithm when varying $R_{min}$ while keeping K equals 1000 and using $\beta_0 = 95\%$. The results show that by decreasing $R_{min}$ from 400 km to 200 km, the protection distance (where the eNodeB is allowed to transmit with the maximum power) is increased from around 67 km to around 230 km. This is because the level of the aggregate interference

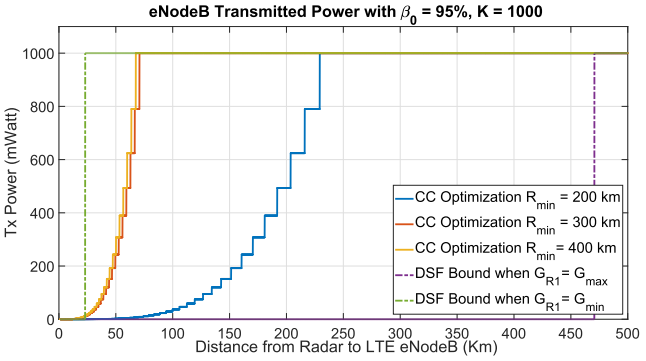


**FIGURE 8.** Chance-constrained optimization algorithm for a different values of $R_{min}$ using K = 1000.

**TABLE 3.** Summary of relative impact of parameters on the results.

| Parameter | Impact |
|---|---|
| Increasing the confidence level ($\beta_0$) | Decreasing the distance at which the eNodeB is allowed to transmit with the maximum power |
| Increasing the total number of eNodeBs ($K$) | Decreasing the distance at which the eNodeB is allowed to transmit with the maximum power |
| Reducing ($R_{min}$), which is the minimum distance the other eNodeBs is allowed with the maximum transmit power level | Decreasing the distance at which the eNodeB is allowed to transmit with the maximum power |

level produced by the other eNodeBs is increased when reducing $R_{min}$.

### D. RESULTS ANALYSIS

To summarize our assumptions, we have limited our analysis to downlink transmission only, where we analyzed the effect of eNodeB transmission on the interference on the radar system. Also we have assumed that interference to the eNodeB is generated for the radar transmission, as there is no mutual interference among the eNodeBs. For the multiple-cell scenario, we also have assumed that all other eNodeBs that are allowed to transmit are transmitting with the maximum power level. To summarize the trends, the performance of the CC optimization algorithm will get affected by the radar transmission power, radar antenna gain, propagation model, and eNodeB antenna gain. Table 3 summarizes the relative impact of the other main parameters on the results of the proposed CC optimization algorithm.

These results are significant, as it provides insightful analysis for the minimum protection distance required between the radar and the LTE-Unlicensed for the two to coexist and operate effectively. For the regulations authorities, these results provide a an accurate analysis for the effect of utilizing power-control mechanism at the secondary users (SU) side. These results suggest a huge improvement to the efficiency of the DFS algorithm by creating multiple detection thresholds, at each one, the SU is allowed to transmit with certain maximum transmission power. Modifying the regulations will greatly increase the number of secondary users that are allowed to share the 5 GHz with the radar systems and will not create any excessive interference at the radar side.

For the LTE, these results affect the eNodeB scheduler, as the scheduler will need to increase the bandwidth allocation to compensate for the reduction in the maximum allowable transmission power.

## VII. CONCLUSION

In this paper, we have proposed a new spectrum sharing mechanism between radar and LTE systems in the unlicensed 5 GHz spectrum. The proposed algorithm is based on a chance-constrained stochastic optimization, which provides a minimum acceptable threshold for both the radar and the LTE systems. For the single-cell scenario, the radar antenna gain and the shadow fading channel are treated as random variables. Doing so, the proposed technique is capable of estimating an eNodeB transmit power that satisfies the radar and UE performance criteria, while significantly decreasing the protection distance between the radar and eNodeB. For the multiple cells scenario, where the optimization problem is formulated for a single eNodeB, the location of the other eNodeBs and the shadow fading channel both are treated as random variable and the stochastic optimization problem was transformed to deterministic one through mathematical analysis. The numerical results after solving the optimization problem for the multiple-eNodeBs scenario clearly show that, even with the existence of hundreds of other eNodeBs, the proposed algorithm still allows the eNodeB to reduce its protection distance to the radar while maintaining acceptable performance for both the radar and LTE systems to coexist. The results should motivate the regulation authorities to reconsider the effectiveness of the current DFS algorithm; a more effective way is to use an adaptive DFS algorithm, in which the cellular system can be allowed to transmit up to a certain power level based on the received level of the radar signal. Doing so will improve the overall capacity for cellular communications without affecting the radar performance.

Future work will further extend the analysis for optimizing the performance for multiple eNodeBs sharing the spectrum with a radar system at the same time, where all the eNodeBs will employ a power control algorithm to maintain the aggregate interferences at an acceptable level for effective radar operation. Future work will also include analyzing the impact of the height of the eNodeB.

## REFERENCES


[1] S. Bhattarai, J.-M. J. Park, B. Gao, K. Bian, and W. Lehr, "An overview of dynamic spectrum sharing: Ongoing initiatives, challenges, and a roadmap for future research," *IEEE Trans. Cogn. Commun. Netw.*, vol. 2, no. 2, pp. 110–128, Jun. 2016.

[2] Y.-C. Liang, K.-C. Chen, G. Y. Li, and P. Mahonen, "Cognitive radio networking and communications: An overview," *IEEE Trans. Veh. Technol.*, vol. 60, no. 7, pp. 3386–3407, Sep. 2011.

[3] Office of the Press Secretary, The White House, Press Release. (Jun. 2013). *Presidential Memorandum: Expanding America's Leadership in Wireless Innovation*. [Online]. Available: https://www.whitehouse.gov/the-press-office/2013/06/14/presidential-memorandum-expanding-americas-leadership-wireless-innovatio

[4] B. J. Evans. Shared Spectrum Access for Radar and Communications (SSPARC). DARPA. Accessed: Dec. 2018. [Online]. Available: https://www.darpa.mil/program/shared-spectrum-access-for-radar-and-communications

[5] M. Labib, V. Marojevic, J. H. Reed, and A. I. Zaghloul, "Extending LTE into the unlicensed spectrum: Technical analysis of the proposed variants," *IEEE Commun. Standards Mag.*, vol. 1, no. 4, pp. 31–39, Dec. 2017.

[6] *Characteristics of and Protection Criteria for Sharing Studies for Radiolocation (Except Ground Based Meteorological Radars) and Aeronautical Radio-Navigation Radars Operating in the Frequency Bands Between 5 250 and 5 850 MHz*, document Rec. ITU-R M.1638-1, Jan. 2015.

[7] M. Labib, V. Marojevic, A. F. Martone, J. H. Reed, and A. I. Zaghloui, "Coexistence between communications and radar systems: A survey," *URSI Radio Sci. Bull.*, vol. 2017, no. 362, pp. 74–82, Sep. 2017.

[8] S. S. Bhat, R. M. Narayanan, and M. Rangaswamy, "Bandwidth sharing and scheduling for multimodal radar with communications and tracking," in *Proc. IEEE 7th Sensor Array Multichannel Signal Process. Workshop (SAM)*, Jun. 2012, pp. 233–236.

[9] A. F. Martone, K. I. Ranney, K. Sherbondy, K. A. Gallagher, and S. D. Blunt, "Spectrum allocation for noncooperative radar coexistence," *IEEE Trans. Aerosp. Electron. Syst.*, vol. 54, no. 1, pp. 90–105, Feb. 2018.

[10] A. F. Martone, K. A. Gallagher, K. Sherbondy, A. Hedden, and C. Dietlein, "Adaptable waveform design for enhanced detection of moving targets," *IET Radar, Sonar Navigat.*, vol. 11, no. 10, pp. 1567–1573, Oct. 2017.

[11] S. Gogineni, M. Rangaswamy, and A. Nehorai, "Multi-modal OFDM waveform design," in *Proc. IEEE Radar Conf. (RadarCon)*, Apr./May 2013, pp. 1–5.

[12] R. Blank and E. L. Strickling, "Evaluation of the 5350–5470 MHz and 5850–5925 MHz bands pursuant to section 6406(b) of the middle class tax relief and job creation act of 2012," U.S. Dept. Commerce, NTIA, Washington, DC, USA, Tech. Rep., Jan. 2013. [Online]. Available: https://www.ntia.doc.gov/files/ntia/publications/ntia_5_ghz_report_01-25-2013.pdf

[13] E. F. Drocella, L. Brunson, and C. T. Glass, "Description of a model to compute the aggregate interference from radio local area networks employing dynamic frequency selection to radars operating in the 5 GHz frequency range," NTIA, Washington, DC, USA, NTIA Tech. Memorandum 09-461, May 2009.

[14] F. Paisana, Z. Khan, J. Lehtomäki, L. A. DaSilva, and R. Vuohtoniemi, "Exploring radio environment map architectures for spectrum sharing in the radar bands," in *Proc. 23rd Int. Conf. Telecommun. (ICT)*, May 2016, pp. 1–6.

[15] J. Um, J. Park, and S. Park, "Multi-antenna-based transmission strategy in 5 GHz unlicensed band," in *Proc. 8th Int. Conf. Ubiquitous Future Netw. (ICUFN)*, Jul. 2016, pp. 651–655.

[16] R. Saruthirathanaworakun, J. M. Peha, and L. M. Correia, "Opportunistic sharing between rotating radar and cellular," *IEEE J. Sel. Areas Commun.*, vol. 30, no. 10, pp. 1900–1910, Nov. 2012.

[17] H. Wang, J. Johnson, C. Baker, L. Ye, and C. Zhang, "On spectrum sharing between communications and air traffic control radar systems," in *Proc. IEEE Radar Conf. (RadarCon)*, May 2015, pp. 1545–1550.

[18] M. Tercero, K. W. Sung, and J. Zander, "Impact of aggregate interference on meteorological radar from secondary users," in *Proc. IEEE Wireless Commun. Netw. Conf. (WCNC)*, Mar. 2011, pp. 2167–2172.

[19] F. Hessar and S. Roy, "Spectrum sharing between a surveillance radar and secondary Wi-Fi networks," *IEEE Trans. Aerosp. Electron. Syst.*, vol. 52, no. 3, pp. 1434–1448, Jun. 2016.

[20] S.-S. Raymond, A. Abubakari, and H.-S. Jo, "Coexistence of power-controlled cellular networks with rotating radar," *IEEE J. Sel. Areas Commun.*, vol. 34, no. 10, pp. 2605–2616, Oct. 2016.

[21] N. N. Krishnan, R. Kumbhkar, N. B. Mandayam, I. Seskar, and S. Kompella, "Coexistence of radar and communication systems in CBRS Bands through downlink power control," in *Proc. IEEE Mil. Commun. Conf. (MILCOM)*, Oct. 2017, pp. 713–718.

[22] S.-J. Kim, N. Y. Soltani, and G. B. Giannakis, "Resource allocation for OFDMA cognitive radios under channel uncertainty," *IEEE Trans. Wireless Commun.*, vol. 12, no. 7, pp. 3578–3587, Jul. 2013.

[23] N. Y. Soltani, S. J. Kim, and G. B. Giannakis, "Chance-constrained optimization of OFDMA cognitive radio uplinks," *IEEE Trans. Wireless Commun.*, vol. 12, no. 3, pp. 1098–1107, Mar. 2013.

[24] Y. J. A. Zhang and A. M.-C. So, "Optimal spectrum sharing in MIMO cognitive radio networks via semidefinite programming," *IEEE J. Sel. Areas Commun.*, vol. 29, no. 2, pp. 362–373, Feb. 2011.

[25] W. W.-L. Li, Y.-J. Zhang, A. M.-C. So, and M. Z. Win, "Slow adaptive OFDMA systems through chance constrained programming," *IEEE Trans. Signal Process.*, vol. 58, no. 7, pp. 3858–3869, Jul. 2010.

[26] E. Dall'Anese, S.-J. Kim, G. B. Giannakis, and S. Pupolin, "Power control for cognitive radio networks under channel uncertainty," *IEEE Trans. Wireless Commun.*, vol. 10, no. 10, pp. 3541–3551, Oct. 2011.
[27] *Evolved Universal Terrestrial Radio Access (E-UTRA); User Equipment (UE) Radio Transmission and Reception (Release 13)*, document 3GPP, TS 36.101, Oct. 2015. [Online]. Available: http://www.3gpp.org/dynareport/36101.htm
[28] K. W. Sung, M. Tercero, and J. Zander, "Aggregate interference in secondary access with interference protection," *IEEE Commun. Lett.*, vol. 15, no. 6, pp. 629–631, Jun. 2011.
[29] A. Papoulis and S. U. Pillai, *Probability, Random Variables, and Stochastic Processes*, 4th ed. Boston, MA, USA: McGraw-Hill, 2002.
[30] M. Pratesi, F. Santucci, and F. Graziosi, "Generalized moment matching for the linear combination of lognormal RVs—Application to outage analysis in wireless systems," in *Proc. IEEE 17th Int. Symp. Pers., Indoor Mobile Radio Commun. (PIMRC)*, Sep. 2006, pp. 1–5.
[31] A. Babaei and B. Jabbari, "Interference modeling and avoidance in spectrum underlay cognitive wireless networks," in *Proc. IEEE Int. Conf. Commun. (ICC)*, May 2010, pp. 1–5.
[32] X. Zhang and M. Haenggi, "A stochastic geometry analysis of inter-cell interference coordination and intra-cell diversity," *IEEE Trans. Wireless Commun.*, vol. 13, no. 12, pp. 6655–6669, Dec. 2014.

**MINA LABIB** received the B.S. degree in electronics and communications engineering from Ain Shams University, Cairo, Egypt, the M.Sc. degree in systems and computer engineering from Carleton University, Ottawa, ON, Canada, and the Ph.D. degree in electrical engineering from Virginia Tech, in 2017. During the Ph.D. degree, he was a Research Assistant with Wireless @ Virginia Tech (the Bradley Department of Electrical and Computer Engineering, Virginia Tech), and he has held internship positions at U.S. Army Research Lab and Qualcomm Technologies, Inc. He has a wide industrial experience, especially in the fields of physical and MAC layer design. He is currently with Qualcomm Technologies, Inc., where he is involved in next-generation wireless technologies. His current research interests include the broad areas of wireless communications, with a particular emphasis on 5G systems, LTE systems, LTE-unlicensed, MIMO, spectrum sharing, game theory, and stochastic optimization. He serves as a reviewer for several international conferences and journals.

**ANTHONY F. MARTONE** received the B.S. degree in electrical engineering from Rensselaer Polytechnic Institute, Troy, NY, USA, in 2001, and the Ph.D. degree in electrical engineering from Purdue University, West Lafayette, IN, USA, in 2007. He joined the U.S. Army Research Laboratory (ARL), Adelphi, MD, USA, in 2007, as a Researcher in the RF Signal Processing and Modeling Branch. He is currently the Sensors and Electron Devices Directorate lead for Cognitive Radar Research, where he is overseeing, directing, and collaborating with multiple universities to address spectrum sharing for radar and communication systems, software defined transceiver control, and adaptive processing techniques. Since joining ARL, he has authored more than 70 journal and conference publications, two book chapters, and holds seven patents. His research interests include sensing through the wall technology, spectrum sharing, and radar signal processing. He has served as a Committee Member for graduate students at The Pennsylvania State University, the Virginia Polytechnic Institute and State University, and Bowie State University. He received the Commanders Award for Civilian Service, in 2011 for his research and development of sensing through the wall signal processing techniques. He is an Associate Editor of the IEEE TRANSACTION ON AEROSPACE AND ELECTRONIC SYSTEMS.

**VUK MAROJEVIC** is currently an Associate Professor in electrical and computer engineering with Mississippi State University, Starkville Campus. His research interests include resource management, vehicle-to-everything communications, physical-layer security, spectrum sharing, software radios, and wireless network virtualization with application to commercial cellular communications, mission-critical networks, and unmanned aircraft systems.

**JEFFREY H. REED** is currently the Willis G. Worcester Professor with the Bradley Department of Electrical and Computer Engineering, Virginia Tech. He is also the Founder of Wireless @ Virginia Tech, and served as the Director, until 2014. He is also the Founding Faculty Member of the Ted and Karyn Hume Center for National Security and Technology and served as the interim Director when founded, in 2010. He is also a Co-Founder of Cognitive Radio Technologies (CRT), a company commercializing of the cognitive radio technologies; Federated Wireless, a company developing spectrum sharing technologies; and for PFP Cybersecurity, a company specializing in security for embedded systems. His book, *Software Radio: A Modern Approach to Radio Design* (Prentice Hall) and his latest textbook *Cellular Communications: A Comprehensive and Practical Guide* (Wiley-IEEE, 2014). In 2005, he became a Fellow to the IEEE for contributions to software radio and communications signal processing and for leadership in engineering education. He is a Past Member CSMAC a group that provides advice to the NTIA on spectrum issues. In 2013, he received the International Achievement Award by the Wireless Innovations Forum. In 2012, he served on the President's Council for the Advisors of Science and Technology Working Group that examine ways to transition federal spectrum for commercial use.

**AMIR I. ZAGHLOUL** received the B.Sc. degree (Hons.) from Cairo University, Egypt, in 1965, the M.A.Sc. and Ph.D. degrees from the University of Waterloo, Canada, in 1973 and 1970, respectively, all in electrical engineering, and the M.B.A. degree from George Washington University, in 1989.

After 24 years at COMSAT Laboratories, performing and directing R&D efforts on satellite communications and antennas, he joined Virginia Tech, in 2001 as a Professor with the Electrical and Computer Engineering Department. In 2008, he was assigned as an IPA from Virginia Tech to the Army Research Lab, where he subsequently switched to full time at ARL, in 2012, maintaining his affiliation with Virginia Tech as a Research Professor. He held positions at the Universities of Waterloo and Toronto, Canada, Aalborg University, Denmark, and Johns Hopkins University, MD, USA. He is currently an ARL Fellow with the Sensors and Electron Devices Directorate (SEDD) of the U.S. Army Research Laboratory, Adelphi, MD, USA.

Dr. Zaghloul is a Fellow of the International Union of Radio Science (URSI), of the Applied Computational Electromagnetics Society (ACES), and an Associate Fellow of The American Institute of Aeronautics and Astronautics (AIAA). He is also the International Chair of Commission C of URSI.